Veterinary Microbiology 233 (2019) 39–46

Contents lists available at ScienceDirect

Veterinary Microbiology

journal homepage: www.elsevier.com/locate/vetmic

Bovine papillomavirus E5 oncoprotein expression and its association with an interactor network in aggresome-autophagy pathway

Sante Roperto[a,*], Valeria Russo[a], Francesca De Falco[a], Chiara Urraro[a], Paola Maiolino[a], Fabio Del Piero[b], Franco Roperto[c]

[a] Dipartimento di Medicina Veterinaria e Produzioni Animali, Università di Napoli Federico II, Napoli, Italy
[b] Department of Pathobiological Sciences, School of Veterinary Medicine, Louisiana State University, USA
[c] Dipartimento di Biologia, Università di Napoli Federico II, Napoli, Italy

ARTICLE INFO

Keywords:
Bovine papillomavirus E5 oncoprotein
Bag3
Dynein
14-3-3γ
Aggresome
eIF2a
synpo2

ABSTRACT

E5 protein, the major oncoprotein of bovine Deltapapillomavirus (BPV), was found to be expressed in 18 of 21 examined urothelial cancers of cattle. E5 oncoprotein was found to interact with p62 which was degraded through the autophagosome-lysosome pathway as well as LC3-II and appeared to be involved in the phosphorylation of the α-subunit of eukaryotic initiation factor 2 (eIF2α). Autophagy was morphologically documented by transmission electron microscope (TEM) through the detection of double-membrane autophagosomes and autolysosomes. Overexpression of Bag3 known to mediate selective autophagy was also demonstrated. Furthermore, Bag3 and BPV E5 oncoprotein were seen to co-localize with dynein and 14-3-3γ, which suggested that Bag3 could be involved in inducing the retrograde transport of BPV E5 along microtubules to aggresomes, perinuclear sites with high autophagic flux. Electron dense perinuclear structures consistent with aggresomes were also documented by TEM in urothelial cancer cells. Finally, Bag3 was found to also interact with synaptopodin 2 (Synpo2), which would seem to contribute to cargo degradation as it has been shown to facilitate autophagosome formation. This study provides mechanistic insights into the potential role(s) of autophagy in BPV disease, which can help to develop future treatment and control measures for BPV infection. Activation of autophagy correlates positively with BPV infection and may play a role in biological behavior of bladder cancer as urothelial carcinomas of cattle are known to be characterized by a relatively low rate of metastasis.

1. Introduction

Bovine papillomaviruses (BPVs) consist of 24 types that are distributed into five genera: Deltapapillomavirus (δPV) (BPV-1, -2, -13, -14), Xipapillomavirus (χPV) (BPV-3, -4, -6, -9, -10, -11, -12, -15, -17, -20, -23, -24), Epsilonpapillomavirus (εPV) (BPV-5, -8), Dyokappapapillomavirus (DyoκPV) (BPV-16, -18, -22), Dyoxipapillomavirus (DyoχPV) (BPV-7). BPV-19 and BPV-21 remain to be classified (http://pave.niaid.nih.gov). Very recently, a new species of BPV has been fully sequenced and referred to as ujs-21015; it has been identified as an additional member of DyoχPV (Ling et al., 2019). Among BPVs, δPVs are considered high risk in association with neoplastic transformation (Daudt et al., 2018). Indeed, bovine δPVs play a central role in cutaneous as well as bladder tumors. In southern Italy, BPV-2 and BPV-13 are the most important infectious agents involved in bladder carcinogenesis in cattle (Roperto et al., 2016). BPV-2 and BPV-13 are known to cause a cross-species infection, and their expression has been shown as responsible for neoplastic and non-neoplastic diseases in small ruminants (Roperto et al., 2018a).

The BPV genome contains several open reading frames (ORFs) in which it is possible to recognize three functional parts: the early (E) genes encode proteins (E1-E7) that are necessary for viral replication and can subvert cellular proliferation, ultimately leading to cell transformation; the late (L) genes encode the structural proteins (L1-L2) that are required for virion assembly and a long control region involved in replication and transcription of viral DNA (Campo, 2003).

The small (40–85 amino acids) δPV E5, believed to be the major oncoprotein of δPVs (Campo et al., 1992; DiMaio and Petti, 2013; Roperto et al., 2010b), is the best studied protein and displays transforming activity via numerous pathways every in the absence of other viral genes (DiMaio and Petti, 2013). E6 of δPVs appears to contribute to cell transformation by its interaction with the focal adhesion protein paxillin. Transforming function of δPV E7 appears to be correlated with its ability to bind to p600 even if E7 by itself is not sufficient to induce

* Corresponding author.
E-mail address: sante.roperto@unina.it (S. Roperto).

https://doi.org/10.1016/j.vetmic.2019.04.021
Received 18 February 2019; Received in revised form 11 April 2019; Accepted 12 April 2019

cell transformation (DeMasi et al., 2007). Recently, E5 oncoprotein has been shown to activate chaperone-associated selective autophagy (CASA) mediated by Bag3, a member of the Bcl-2 associated athanogene protein family (Roperto et al., 2018b).

Autophagy is a process by which cytoplasmic components, including macromolecules and organelles, are degraded by the lysosome (Mizushima and Levine, 2010). There are at least three different types of autophagy: macroautophagy (hereafter referred to as autophagy) characterized by delivery of cytosolic contents to the lysosome by autophagosomes, microautophagy where the cytosolic contents are engulfed by direct invagination of the lysosomal membranes and chaperone-mediated autophagy (CMA), that is a lysosomal pathway responsible for the degradation of cytosolic proteins that are selectively targeted to lysosomes and translocated into the lysosomal lumen through the coordinated action of chaperones (Dice, 2007).

The aggresome-autophagy pathway has emerged as another defense mechanism for selective clearance of toxic proteins, including viral proteins (Jia et al., 2014). Through dynein-mediated retrograde transport, a large variety of selective cargoes are transported to the negative end of a microtubule, forming a larger aggregate, a so-called aggresome (Park et al., 2018). Several adaptor proteins mediate recruitment of cytoplasmic dynein and are involved in the retrograde movement of cargoes along microtubules (McKenney et al., 2014; Park et al., 2017). Bag3 appears to be a player involved in different processes that are crucial for protein homeostasis and for proteotoxicity mitigation (Rapino et al., 2014; Klimek et al., 2017), being a powerful regulator of selective autophagy (Gamerdinger et al., 2011a). Bag3 is directly associated with the microtubular motor dynein and mediates the selective transport of cargoes to the aggresome (Behl, 2011; Gamerdinger et al., 2011b; Behl, 2016; Guilbert et al., 2018). It is believed that Bag3 may physically interact with and act in concert with several adaptor molecules for efficient aggresome formation (Park et al., 2017).

The aim of the present paper is to report, in naturally occurring bladder cancer of cattle, a mechanistic study about the expression of bovine δPV E5 oncoprotein responsible for an abortive infection resulting in urothelial cell transformation and its association with a not previously reported, elaborated network of interactors mediated by Bag3 in aggresome-autophagy pathway.

2. Materials and methods

2.1. Ethics statement

In this study we did not perform any animal experiments and no ethics approval is required. All samples were collected post-mortem. The animals were slaughtered following a mandatory clinical antemortem examination as required by European Union legislation.

2.2. Tumor samples

Neoplastic urothelial samples from twenty-one cows clinically suffering from chronic enzootic hematuria were collected after bladder tumors had been identified by post-mortem examination with the permission of the medical authorities. Fifteen mucosa samples of the urinary bladder were also collected from healthy cows. Both neoplastic and non-neoplastic bladder mucosa were divided into several parts that were then fixed in 10% buffered formalin for microscopic investigation as well as in 4% glutaraldehyde in 0.1 M phosphate buffer (pH 7.4) for 2–3 h for transmission electron microscopy or immediately frozen in liquid nitrogen, stored at −80 °C for subsequent molecular biological analysis.

2.3. Histology and immunohistochemistry

The tissues fixed in 10% buffered formalin were routinely paraffin embedded. Histologic diagnosis was assessed on 5-μm-thick hematoxylin-eosin (HE)–stained sections using morphologic criteria previously suggested (Roperto et al., 2010a). Non-neoplastic and neoplastic bladder mucosa were tested in parallel. For E5 and p-eIF2α detections, immunohistochemical staining was carried out using a polymer detection system and an avidin-biotin-peroxidase complex (ABC) method, respectively. Briefly, paraffin sections were deparaffinized in xylene and rehydrated through a graded alcohol series. Antigen retrieval for both BPV E5 and p-eIF2α was performed by pretreating slides with microwave heating (twice for 5 min each at 700 W) in 10 mM sodium citrate pH 6.0. After allowing the slides to cool, they were rinsed three times with phosphate buffered saline (PBS, pH 7.4, 0.01 M), then covered for 20 min at room temperature with peroxidase blocking solution (SP-6000) (Vector Laboratories Inc., CA, USA) to quench endogenous peroxidase activity. For E5 detection, sections were incubated for 1 h at room temperature with 2.5% normal goat serum (MP-7451) (Vector Laboratories Inc., CA, USA) for blocking unspecific staining. A rabbit polyclonal anti-E5 antiserum recognizing the C-terminal 14 amino acids of the BPV E5 proteins (a kind gift by Prof. DiMaio, Yale University, New Haven, USA), diluted at 1 in 1000, was applied at room temperature for 1 h in a humid chamber. Slides were washed three times with PBS, then incubated with ImmPRESS peroxidase polymer anti-rabbit IgG reagent made in goat (MP-7451) (Vector Laboratories Inc., CA, USA) at room temperature for 30 min. For p-eIF2α immunostaining, the sections were incubated with 20% normal goat serum (S-1000) (Vector Laboratories, Inc., CA, USA) for 1 h at room temperature. A rabbit polyclonal anti-p-eIF2α (Ser52) (sc-101670) (Santa Cruz Biotechnology Inc., CA, USA), diluted at 1 in 50, was applied at room temperature for 1 h in a humid chamber, and, after washing with PBS, slides were incubated for 30 min with a biotinylated secondary anti-rabbit antibody made in goat (BA-1000) (Vector Laboratories Inc., CA, USA), diluted at 1 in 200. Successively, sections were incubated with Vectastain Elite ABC-HRP kit (PK-6100) (Vector Laboratories Inc., CA, USA) at room temperature for 30 min. Color development was obtained for both immunohistochemical staining by treatment with ImmPACT DAB peroxidase substrate (SK-4105) (Vector Laboratories Inc., CA, USA) for 2–5 min. Sections were counterstained with Mayer's hematoxylin. The anti-E5 rabbit polyclonal antiserum specificity was also shown by using sections from the same pathological tissue samples where the antiserum was omitted and replaced by a normal rabbit serum (S-5000) (Vector Laboratories Inc., CA, USA). The rabbit polyclonal anti-p-eIF2α specificity was demonstrated by using sections from the same pathological tissue samples where the primary antibody was omitted and replaced by corresponding species- and isotype-matched immunoglobulins (IgG) (P120-201) (Bethyl Laboratories., Inc., TX, USA) at same concentrations.

2.4. Confocal microscopy

All non-neoplastic and neoplastic samples from bladder mucosa of cattle were tested simultaneously. Paraffin sections, after dewaxing and rehydrating, were pre-treated with microwave heating (twice for 5 min each at 700 W) in 10 mM sodium citrate pH 6.0. Slides were rinsed three times in PBS and then incubated with 20% donkey serum for 1 h for blocking nonspecific staining. A double-labeling indirect immunofluorescence staining was performed to detect colocalization of BPV E5 and Bag3, BPV E5 and dynein, BPV E5 and p62, BPV E5 and Hsc/Hsp70. The following primary antibodies were used: a purified polyclonal sheep anti-BPV E5 (a kind gift by Dr. L. Nasir, Glasgow University), diluted at 1 in 25, a monoclonal mouse anti-Bag3 (AC-1) (Biouniversa s.r.l., AV, Italy), (1 in 30), a monoclonal mouse anti-dynein IC1/2, cytosolic (sc-166130) (Santa Cruz Biotechnology, TX, USA), (1 in 25), a monoclonal mouse anti-p62 (sc-28359) (Santa Cruz Biotechnology, TX, USA), (1 in 50), a monoclonal mouse anti-Hsc/Hsp70 (sc 7298) (Santa Cruz Biotechnology, TX, USA), (1 in 50). All primary antibodies were applied overnight at +4 °C in a humid chamber. Alexa Fluor 488 donkey anti-sheep secondary antibody

(Thermo Fisher Scientific, MA, USA) (A11015), diluted at 1 in 50, was applied for BPV-E5 labeling and Alexa Fluor 546 donkey anti-mouse secondary antibody (Thermo Fisher Scientific, MA, USA) (A10036), diluted at 1 in 50, was applied for Bag-3, dynein IC1/2, p62 and Hsc/Hsp70 labelling. Both fluorescent secondary antibodies were applied for 2 h at room temperature in a humid chamber. Slides were mounted with Fluoromont aqueous medium. For observation and photography, a laser scanning confocal microscope LSM-510 (Zeiss, Göttingen, Germany) was used.

2.5. Transmission electron microscope (TEM)

Non-neoplastic and neoplastic bladder mucosa were immediately fixed in 4% glutaraldehyde in 0.1 M phosphate buffer (pH 7.4) for 2–3 h. They were washed (20 min 5 times) and post fixed in 1% OsO_4 in the same buffer for 1 h. They were washed again in 0.1 M phosphate buffer (pH 7.4) and then dehydrated in graded alcohol and embedded in Agar Low Viscosity Resin (AGR 1078) (Agar Scientific Limited, Essex, England). Semi-thin sections (400 nm) were obtained by an EM UC6 ultramicrotome (Leica Microsystems) and were stained with 1% toluidine blue in water solution and examined by light microscopy. Ultrathin sections (60–70 nm) obtained were collected onto 300-mesh grids coated with formvar and counterstained with lead citrate and uranyl acetate. The sections were observed with a JEOL JEM-1011 transmission electron microscope (JEOL, Tokyo, Japan) equipped with a thermionic tungsten filament and operated at an acceleration voltage of 100 kV. Images were taken using a Morada cooled slow-scan CCD camera (3783 × 2672 pixels) and micrographs were taken with iTEM software (Olympus Soft Imaging System GmbH, Munster, Germany).

2.6. Western blot analysis

Samples of the neoplastic and non-neoplastic bladder mucosa were lysed in RIPA buffer (50 mMTris-HCl pH 7.5, 1% Triton X-100, 150 mM NaCl, 2 mM PMSF, 1.7 mg/ml Aprotinin, 50 mMNaF, and 1 mM sodium orthovanadate) and clarified by centrifugation. The protein concentration was measured using the Bradford assay (Bio-Rad, CA, USA). For Western blotting, 50 µg of protein lysate were heated at 90 °C in 4X premixed Laemmli sample buffer (Bio-Rad, CA, USA), separated by SDS-PAGE and transferred to nitrocellulose membranes (GE Heatlhcare, LC, UK). Membranes were blocked with Tris buffer saline and 0.1% Tween 20 (TBST) containing 5% bovine serum albumin for 1 h at room temperature and were then incubated overnight at 4 °C with primary antibodies diluted in TBST. The following antibodies were used: a rabbit polyclonal anti-E5 antiserum (a kind gift from prof. Di Maio), a rabbit polyclonal anti-Bag3 (27 F 189C3) (Biouniversa s.r.l., AV, Italy), a mouse monoclonal anti-14-3-3γ (sc-398423) (Santa Cruz Biotechnology, TX, USA), a mouse monoclonal anti-dynein IC1/2, cytosolic (sc-166130) (Santa Cruz Biotechnology, TX, USA), a mouse monoclonal anti-β actin (sc-47778) (Santa Cruz Biotechnology, TX, USA), a mouse monoclonal anti-p62 (sc-28359) (Santa Cruz Biotechnology, TX, USA), a rabbit polyclonal anti-elF2α (sc-11386) (Santa Cruz Biotechnology, TX, USA), a rabbit polyclonal anti-p-elF2α (Ser52) (sc-101670) (Santa Cruz Biotechnology, TX, USA), a rabbit polyclonal anti-LC3 (NB100-2220) (Novus Biologicals, CO, USA), a rabbit polyclonal anti-synpo2 (orb75524) (Biorbyt, CAM, UK). Membranes were washed three times with TBST, incubated for 1 h at room temperature with a goat anti-rabbit (170–6515) and goat anti-mouse (170–6516) (Bio-Rad, CA, USA) HRP-conjugated secondary antibodies diluted at 1 in 2000 in TBST, and washed three times with TBST. Immunoreactive bands were detected using Western Blotting Luminol Reagent (sc-2048) (Santa Cruz Biotechnology, TX, USA) and ChemiDoc XRS Plus (Bio-Rad, CA, USA). Images were acquired with Image Lab Software version 2.0.1 (Bio-Rad, CA, USA).

2.7. Immunoprecipitation

Neoplastic and non-neoplastic bladder mucosa were lysed in immunoprecipitation buffer containing 50 mM Tris-HCl (pH 7.5), 1% (v/v) Triton X-100, 150 mM NaCl, 2 mM PMSF, 1.7 mg/ml Aprotinin, 50 mM NaF, and 1 mM sodium orthovanadate. Proteins (1 mg) were immunoprecipitated by using the above reported antibodies: an anti-E5 (a kind gift by prof. DiMaio, Yale University, New Haven, USA), an anti-p62 (sc-28359), an anti-eIF2α (sc-11386), an anti-p-eIF2α (Ser52) (sc-101670), an anti-dynein IC1/2 cytosolic (sc-166130), an anti-14-3-3γ (sc-398423); an anti-Bag3 (27 F 189C3), an anti-LC3 and 30 µl of Protein A/G-Plus Agarose (sc-2003) (Santa Cruz Biotechnology, TX, USA) overnight at 4 °C. Immunoprecipitates were washed four times in complete lysis buffer (above), and separated on polyacrylamide gels. Following transfer of proteins, membranes were blocked for 1 h at room temperature in 5% bovine serum albumin, incubated with respective primary antibodies overnight at 4 °C. After three washes in Tris-buffered saline, membranes were incubated with respective secondary antibodies for 1 h at room temperature. Chemiluminescent signals were then developed with Western Blotting Luminol Reagent (Santa Cruz Biotechnology, TX, USA) and detected by the ChemiDoc XRS Plus gel documentation system (Bio-Rad, CA, USA).

2.8. RNA extraction and Reverse transcription (RT)-PCR

Total RNA was extracted from neoplastic and non-neoplastic bladder mucosa by RNeasy Mini Kit (Qiagen TM, ME, DE) in according to the manufacturer's instructions. All RNA samples were analyzed spectrophotometrically on a Nanodrop (Nanovue plus, GE healthcare, IL, USA) and DNase treated by RNase-free DNase I Fermentas Life Sciences (Thermo Fisher Scientific, MA, USA) according to the manufacturer's instructions. Five hundred nanograms of the total RNA was used to generate the first strand of cDNA by the QuantiTect Reverse Transcription Kit (205311, Qiagen TM, ME, DE) in according to the manufacturer's instructions. PCR was performed with a specific primer set designed by the Primer3 online tool for bovine p62 gene, BPV-2 E5 and BPV-13 E5, using β-actin as a control. The following primers were used: p62 forward 5'-AGGACTGAAGGAAGCTGCAC-3', p62 reverse 5'-GAGAGGGACTCAATCAGCCG-3'; BPV-2 E5: forward 5′- CACTGCCATT TGTTTTTTTC-3′, reverse 5′- GGAGCACTCAAAATGATCCC -3′; BPV-13 E5: forward 5′- CACTGCCATTTGGTGTTCTT -3′, reverse 5′- AGCAGTC AAAATGATCCCAA-3′, ß-actin forward 5′-TAGCACAGGCCTCTCGCCT TCG-3′, reverse 5′-GCACATGCCGGAGCCGTTGT-3′. Conditions for PCR were: 94 °C for 5 min, 40 cycles of 95 °C for 30 s, 58 °C for 30 s and 72 °C for 30 s.

2.9. Sequence analysis

PCR products from cDNA were purified using a Qiaquick PCR Purification Kit (Qiagen TM, ME, DE) and bidirectionally sequenced using a BigDye_Terminator v1.1 Cycle Sequencing Kit (Applied Biosystems, CA, USA) following the manufacturer's recommendations. Sequences were dye-terminator removed by DyeEx_2.0 spin kit (Qiagen TM, ME, DE) and run on a 3500 Genetic Analyser (Applied Biosystems, CA, USA). Electropherograms were analyzed using Sequencing Analysis v5.2 and Sequence Scanner v1.0 software (Applied Biosystems, CA, USA). The sequences obtained were compared to others in GenBank using the BLAST program.

2.10. Real time RT-PCR

To perform real time RT-PCR analysis, total RNA and cDNA from neoplastic and non-neoplastic bladder mucosa were produced as previously described (Roperto et al., 2018a). Real-time RT-PCR was performed on a Bio Rad CFX Connect™ Real Time PCR Detection System (Bio Rad Hercules, CA, USA) using iTAq Universal SYBR® Green

Supermix (Bio Rad Hercules, CA, USA). Each reaction was set in triplicate and the primers used for bovine p62 were the same of RT-PCR. The thermal profile for the PCR was 95 °C for 10 min, 40 cycles of 94 °C for 15 s, 58 °C for 30 s, followed by melting curve. The relative quantification (RQ) was calculated by using CFX Manager™ software, based on the equation $RQ = 2^{-\Delta\Delta Cq}$, where Cq is the quantification cycle to detect fluorescence. Cq data were normalized to the reference β-actin gene (forward: 5′- TAGCACAGGCCTCTCGCCTTCGT-3′, reverse 5′-GCA CATGCCGGAGCCGTTGT-3′).

2.11. Statistical analysis

Results are presented as means ± SD. The different expression of protein content in non-neoplastic and neoplastic bladder samples was assessed by one-way ANOVA, followed by Student's *t*-test for significant differences between the mean values of protein content using GraphPad PRISM software version 5 (GraphPad Software, CA, USA). A P value ≤ 0.05 was considered to indicate statistical significance.

3. Results

3.1. Microscopic patterns of tumors and virological findings

Fourteen of the twenty-one tumors were diagnosed as papillary carcinomas (10 high-grade and 4 low-grade) and two as papillary urothelial neoplasms of low malignant potential (PUNLMPs). The remaining five were invasive carcinomas (3 high-grade and 2 low-grade) (Table 1). Virological findings were characterized by the expression of BPV-2 and BPV-13 as unveiled through detection of E5 transcripts by RT-PCR composed of 154 and 153bp, respectively (Supplemental Fig. S1) and E5 oncoprotein by immunohistochemical analysis (Supplemental Fig. S2). Neither BPV E5 transcripts nor E5 protein expression were detected in any of the non-neoplastic bladder samples.

3.2. Phosphorylation of the α-subunit of eukaryotic initiation factor eIF2α and expression of LC3II and p62 as autophagy markers

BPV E5 is known to be characterized by an endoplasmic reticulum (ER) tropism (Schlegel et al., 1986), which impairs the balance of ER in protein-folding homeostasis thus causing ER stress (Venuti et al., 2011). ER stress results in phosphorylation of eukaryotic initiation factor2α (eIF2α) involved in signaling pathways leading to cellular adaption to stress, known as the "integrated stress response (ISR) program" (Ron and Harding, 2012). Although phosphorylation of eIF2α plays a central role in stress-induced autophagy, the mechanisms of stress-induced regulation of autophagy by virus infection are not well understood (Tallóczy et al., 2002; Lee et al., 2018).

In an attempt to gain mechanistic insights into the role(s) of eIF2α in papillomavirus-associated bladder cancers, we performed immunoblot analysis in non-neoplastic and neoplastic bladder mucosa infected by BPVs. Western blot examination unveiled expression of total eIF2α without any statistically significant differences in neoplastic cells in comparison with non-neoplastic cells (Fig. 1). Furthermore, immunoblot analysis detected a phosphorylated component of eIF2a both in neoplastic and non-neoplastic cells. However, a statistically significant increase of the eIF2α phosphorylation was evident in cancer bladder mucosa (Fig. 1). The remarkable increase of this specific component in neoplastic mucosa in comparison with non-neoplastic mucosa was also demonstrated by immunohistochemical investigations (Supplemental Fig. S3).

eIF2α phosphorylation induces important signs of autophagy including LC3 lipidation (as indicated by the conversion of LC3I in LC3II) and degradation of p62, a stress-inducible cellular protein. As p62 has an LC3-interacting region (LIR) and functions as a selective autophagy receptor for degradation of ubiquitinated substrates (Katsuragi et al., 2015; Shen et al., 2012), we explored how these autophagy markers were expressed in urothelial cells infected by BPVs. Herein we showed, by co-immunoprecipitation studies, that p62 protein bound to BPV E5 oncoprotein as western blot analysis detected p62 in mucosa samples immunoprecipitated by E5 (Fig. 2). These molecular findings were confirmed morphologically as E5 and p62 were found to be colocalized by confocal microscope (Supplemental Fig. S4). Then we investigated the expression of p62 by immunoblot analysis which revealed reduced, statistically significant, levels of the protein in cancer mucosa only (Fig. 3). As p62 protein is selectively degraded through autophagy-lysosomal pathway (Pankiv et al., 2007; Jaakkola and Pursiheimo, 2009; Ichimura and Komatsu, 2010), we next performed a real time RT-PCR on p62 cDNA which detected no significant transcript differences in cancer mucosa in comparison with non-neoplastic mucosa (Fig. 3). Altogether, our results suggest that p62 protein could be selectively degraded by autophagy. Therefore, we studied the potential relationship between p62 and LC3, an enhanced conversion into the lipidated component of which has been documented in urothelial cancer cells infected by BPVs (Roperto et al., 2018b). p62 was found to interact with

Table 1
Histologic diagnosis of δPV-associated urothelial carcinomas. LG = Low- grade; HG = High- grade; + = presence of E5 cDNA; - = absence of E5 cDNA.

Case number	Microscopic patterns	BPV-1 E5 cDNA	BPV-2 E5 cDNA	BPV-13 E5 cDNA	BPV-14 E5 cDNA
1	Papillary urothelial neoplasm of low malignant potential (PNULMP)	–	+	–	–
2	Papillary urothelial neoplasm of low malignant potential (PNULMP)	–	–	+	–
3	LG Papillary urothelial carcinoma	–	+	–	–
4	LG Papillary urothelial carcinoma	–	–	+	–
5	LG Papillary urothelial carcinoma	–	–	+	–
6	LG Papillary urothelial carcinoma	–	+	+	–
7	HG Papillary urothelial carcinoma	–	–	–	–
8	HG Papillary urothelial carcinoma	–	+	–	–
9	HG Papillary urothelial carcinoma	–	+	–	–
10	HG Papillary urothelial carcinoma	–	+	+	–
11	HG Papillary urothelial carcinoma	–	+	+	–
12	HG Papillary urothelial carcinoma	–	–	+	–
13	HG Papillary urothelial carcinoma	–	+	–	–
14	HG Papillary urothelial carcinoma	–	+	–	–
15	HG Papillary urothelial carcinoma	–	–	–	–
16	HG Papillary urothelial carcinoma	–	+	+	–
17	LG Invasive urothelial carcinoma	–	–	–	–
18	LG Invasive urothelial carcinoma	–	+	+	–
19	HG Invasive urothelial carcinoma	–	+	+	–
20	HG Invasive urothelial carcinoma	–	–	+	–
21	HG Invasive urothelial carcinoma	–	+	+	–

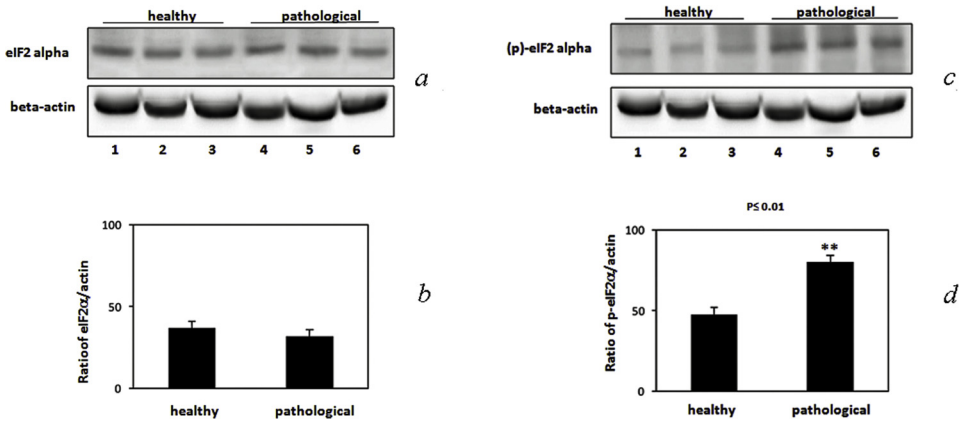

Fig. 1. (a) Total eIF2α detected by western blot analysis in healthy (lanes 1–3) and representative bladder cancer samples (lanes 4–6). Actin protein levels were detected to ensure equal protein loading. (b) Densitometric analysis showing no statistically significant differences in total eIF2α expression between non-neoplastic and neoplastic bladder mucosa. (c) Phosphorylated eIF2α detected by western blot analysis in non-neoplastic (lanes 1–3) and representative neoplastic urothelial samples (lanes 4–6). (d) Actin protein levels were detected to ensure equal protein loading. Densitometric analysis showing statistically significant differences in expression of phosphorylated eIF2α component between non-neoplastic and neoplastic urothelial samples (** $p < 0.01$).

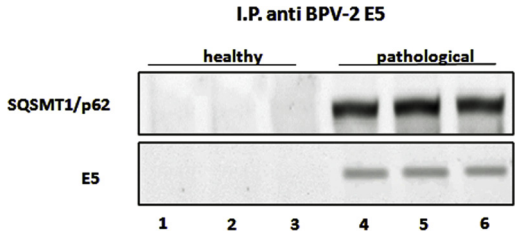

Fig. 2. p62 protein western blot analysis in immunoprecipitated samples by BPV E oncoprotein in healthy (lanes 1–3) and representative neoplastic urothelial samples (lanes 4–6). p62 was detected in urothelial cancer cells only (lanes 4–6).

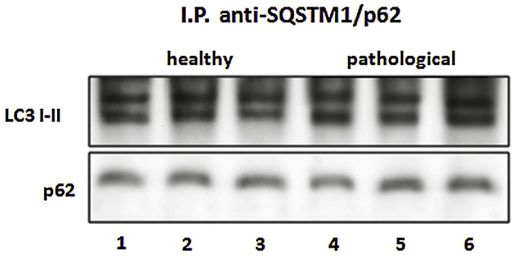

Fig. 4. Western blot analysis detected LC3 protein in samples immunoprecipitated by p62.

LC3 protein since the latter was detected by immunoblot analysis in immunoprecipitated complex by p62 (Fig. 4). These data support the assumption that p62, after binding BPV E5, known to be ubiquitinated by STUB1/CHIP (Roperto et al., 2018a), is degraded by autophagy through the autophagosome-lysosome pathway in urothelial cancer cells. Ultrastructural findings appeared to corroborate our assumption as scattered autophagosomes and autolysosomes were more numerous in urothelial cancer cells rather than in non-neoplastic urothelial cells (Fig. 5).

3.3. Bag3 expression and its interaction with the cytoplasmic dynein and 14-3-3γ proteins

CASA mediated by Bag3 was found to be activated in E5 oncoprotein-expressing urothelial cancer cells (Roperto et al., 2018b). CASA complex was composed of molecular chaperones Hsc/Hsp70 and HspB8 and the co-chaperones Bag3 and STUB1/CHIP (Roperto et al., 2018a). It is believed that at least three cellular adaptors are involved in the selective recognition of aberrant and/or non native proteins degraded by autophagy (Park et al., 2017). One of them is a Bag3-containing chaperone complex (Park et al., 2018). It has been suggested that Bag3 in concert with the 14-3-3γ protein mediates the association of this complex with the dynein complex and thereby promotes intracellular trafficking of protein cargos and their transport to the aggresome (Behl, 2016; Sturnër and Behl, 2017). In urothelial neoplastic mucosa, in anti-Bag3 immunoprecipitated samples, western blot detected the presence of dynein and 14-3-3γ protein as well (Fig. 6). We next investigated whether E5 is a partner of dynein and 14-3-3γ proteins. We immunoprecipitated by an anti-E5 antibody and revealed the

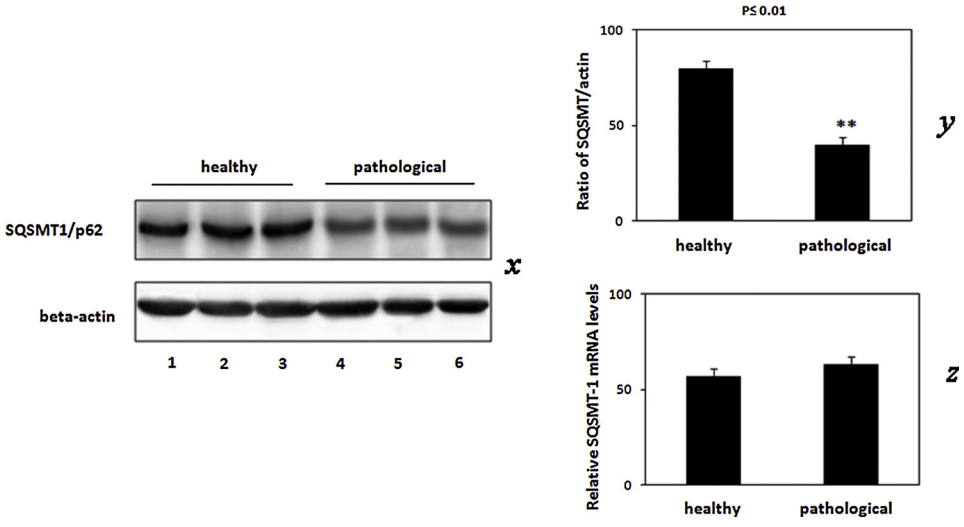

Fig. 3. (x) p62 protein detected by western blot analysis in healthy (lanes 1–3) and bladder cancer samples (lanes 3–6). (y) Actin protein levels were detected to ensure equal protein loading. A statistically significant decrease of the protein was evident in neoplastic urothelial cells (** $p < 0.01$). (z) Real time RT-PCR showing no significant p62 transcript differences between healthy and urothelial cancer cells.

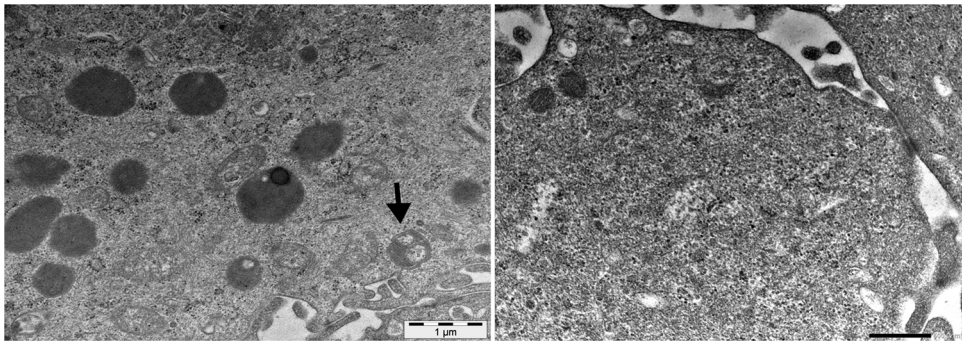

Fig. 5. Left: Ultrastructural findings characterized by scattered autophagosomes and autolysosomes in urothelial cancer cells. Notice also a mitophagosome (arrow). Right: Ultrastructural features seen in the cytoplasm of normal urothelial cells.

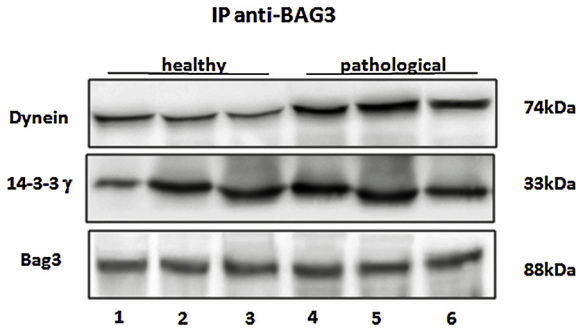

Fig. 6. Western blot analysis of dynein and 14-3-3 γ proteins in healthy (lanes 1–3) and representative urothelial cancer samples (lanes 4–6) in Bag-3 immunoprecipitates.

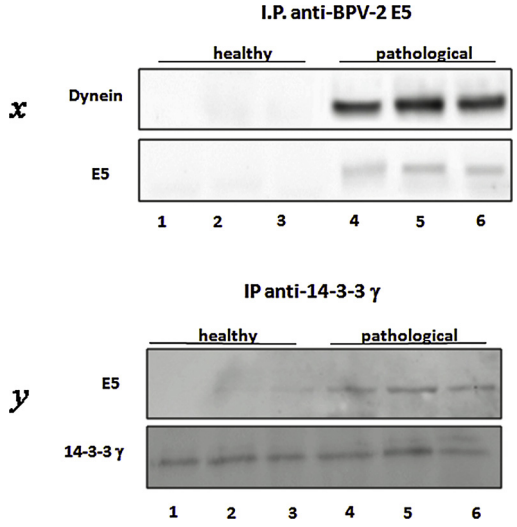

Fig. 7. (x) Dynein detected by western blot in immunoprecipitates by BPV E5 in neoplastic urothelial cells (lines 4–6). (y) BPV E5 detected by western blot analysis in neoplastic urothelial cells (lines 4–6) in samples immunoprecipitated by 14-3-3γ protein.

presence of dynein by immunoblot analysis (Fig. 7). Then, we immunoprecipitated by an anti-14-3-3γ antibody and detected the presence of E5 by western blot (Fig. 7). Morphologically, colocalization of E5/Bag3, E5/dynein and E5/Hsc/Hsp70 complexes was shown by confocal microscopy (Supplemental Figs. S5, S6 and S7). Taken together these morphological and molecular findings are consistent with mechanistic explanation that 14-3-3γ may serve as a molecular adaptor that couples Bag3-Hsc/Hsp70-associated viral cargo to the dynein motor and thereby facilitates its transport to the aggresome. Transmission electron microscope (TEM) revealed perinuclear electron dense features consistent with aggresomal structures (Supplemental Fig. S8).

3.4. Bag3, Synaptopodin 2 (Synpo2) and LC3 interaction

It has been suggested that interaction between Bag3 and Synpo2, a cytoskeleton adaptor protein which acts as a tumor suppressor in the human bladder, plays a crucial role for autophagosome formation in mechanically strained cells during the CASA pathway (Ulbricht et al., 2013). To explore whether similar potential cooperation took place in naturally occurring tension-induced autophagy of bovine bladder, we first documented by western blot analysis the presence, not previously reported, of Synpo2 in healthy and neoplastic bovine bladder mucosa (Fig. 8). Furthermore, Synpo2 and LC3 were detectable in immunoprecipitated complexes by Bag3, known to contain the CASA client and the CASA-mediating ubiquitin adaptor p62 (Fig. 8). LC3 protein was also detected in immunoprecipitated complexes by Synpo2. Altogether these molecular findings are consistent with the assumption that Bag3 and Synpo2 could be involved in the formation of autophagosome membranes, to which LC3 protein is specifically targeted, in urothelial cancer cells infected by BPVs from naturally occurring bladder tumors of cattle.

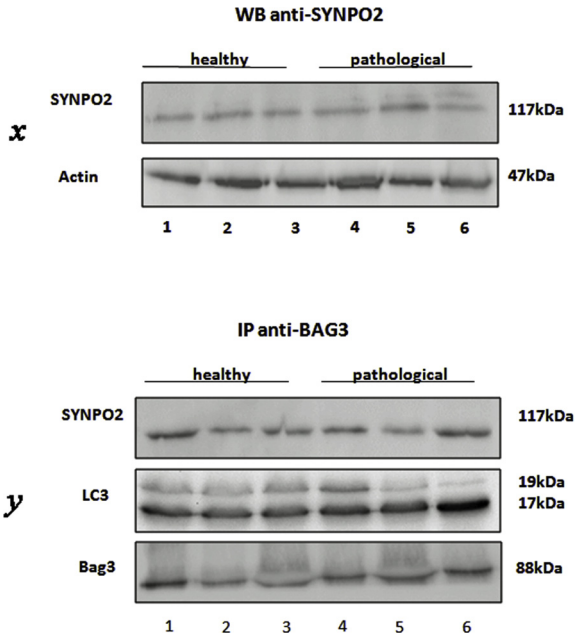

Fig. 8. (x) Western blot analysis of Synpo2 protein. Non-neoplastic (lanes 1–3) and representative bladder cancer samples (lanes 4–6). Actin protein levels were detected to ensure equal protein loading. (y) Synpo2 and LC3 proteins detected by immunoblot analysis in Bag3 immunoprecipitates.

4. Discussion

This is the first study in veterinary medicine describing the association of BPV E5 oncoprotein with a network of interactors, never investigated before, involved in the aggresome-autophagy pathway in bladder cancer of cattle. Of note, CASA complex has been shown to be activated in urothelial neoplastic cells infected by BPVs (Roperto et al., 2018b). Molecular and morphological findings of this mechanistic study are consistent with the assumption that Bag3-containing chaperone complex is responsible for the selective recognition of BPV E5 oncoprotein. Therefore, Bag3 may play a role, in concert with the 14-3-3γ and dynein, in mediating trafficking and transport of E5 oncoprotein to the aggresome, where it recruits p62 to the chaperone complex which ultimately leads to client degradation via autophagosome-lysosome pathway. HspB8 and CHIP, that are overexpressed in urothelial cancer cells of cattle (Roperto et al., 2018a) as well as synpo2 are known to facilitate both recognition of cargo, recruitment of autophagy receptor for ubiquitinated cargo, autophagosome formation and fusion of autophagosome and lysosome (Kettern et al., 2011; Ulbricht et al., 2013; Li et al., 2017; Guilbert et al., 2018).

It is plausible that papillomavirus-induced ER stress is required for autophagy activation via phosphorylation of eIF2α in urothelial cancer cells of cattle. It is also possible that HspB8-Bag3 overexpression, a peculiar feature of bovine bladder carcinoma (Roperto et al., 2018a), could be an additional/alternative route involved in eIF2α phosphorylation. It is worthwhile to remember that it has been suggested that viral infections upregulate HspB8-Bag3 complex which in turn, after recognizing viral proteins, phosphorylates eIF2α (Carra et al., 2008; Carra, 2009; Carra et al., 2009). Recently, GCN2 (general control nonderepressible-2), a kynase responsible for phosphorylation of eIF2α has been shown to be activated by viral infection (Donnelly et al., 2013). Herein, we provide evidence that the phosphorylation of eIF2α is greater in urothelial cancer cells infected by papillomavirus than urothelial cells from non-infected healthy cattle. Induction of eIF2α phosphorylation could result in autophagy stimulation since it facilitates LC3 lipidation and autophagic degradation of p62 (Shen et al., 2012). Therefore, eIF2α phosphorylation and autophagy induction could be two mechanistically linked events in papillomavirus-induced urothelial cancer cells of cattle. In this context, it is worth noting that some oncoproteins of human PV are known to phosphorylate eIF2α (Kazemi et al., 2004).

Since it has been shown that eIF2α phosphorylation plays a central role in the virus life cycle (Choi et al., 2018; Lee et al., 2018), it is also possible that eIF2α phosphorylation is involved in viral replication. This assumption is consistent with *δ*PV productive infections detected in the urothelial cancer cells of cattle (Roperto et al., 2013).

There are many conflicting results about the role of PVs in autophagy; however, recent studies show that human PV infectivity may be mediated by autophagy (Sannigrahi et al., 2015). We demonstrated that selective autophagy is activated in urothelial cancer cells infected by bovine δPVs. However, additional studies are needed to gain insights into the relationship between bovine PV and autophagy. Our findings reported here and in other papers (Roperto et al., 2018b) are very different from autophagy findings observed in human PV infection (Griffin et al., 2013; Surviladze et al., 2013; Mattoscio et al., 2018). Indeed, it is believed that autophagy is strongly impaired by being knocked down and/or inhibited in malignancies mediated by human PV infection such as cervical cancer (Li et al., 2015), head and neck (Sannigrahi et al., 2015) and anal neoplasia (Carchman et al., 2016).

Urothelial carcinomas of cattle are known to be characterized by a relatively low rate of metastasis (8–10%) (Pamukcu, 1974; Roperto et al., 2010a). Although metastasis is a multifactorial process, we do not exclude that the activation of autophagy by BPVs in bladder cancer of cattle could be an additional factor that correlates positively with biological behavior of urothelial cancer caused by BPV infection. It has been suggested that the impairment of the autophagy machinery promotes progression of many malignancies mediated by human PVs (Wang et al., 2014; Mattoscio et al., 2018). Accordingly, as improved autophagy correlates with tumor suppression, its downregulation by viral infection may facilitate cancer development (Choi et al., 2018).

Finally, a role of autophagy in infection and immunity is emerging more and more clearly (Deretic et al., 2013). It is conceivable that the activated autophagy may coordinate adaptive immunity against BPV infection in urothelial cancer cells as lymphocyte responses are known to be peculiar immunological features of urothelial carcinomas of cattle (Roperto et al., 2010a; Maiolino et al., 2013).

5. Conclusion

Autophagy is believed to be a double-edged sword during viral infection (Choi et al., 2018). Our study supports the idea that E5 oncoprotein of bovine Deltapapillomavirus interacts with a network of protein interactors responsible for an activation of autophagy in urothelial cells infected by BPVs. Many pathways are still unknown. Further research is needed to clarify the detailed molecular mechanisms by which autophagy in general and selective autophagy in particular, i.e. mitophagy, can be responsible for immunity against papillomavirus infections and pathogenesis. A better understanding of the mechanisms involved in oncogenesis of bovine papillomavirus can help to develop future treatment and control measures for BPV or even for human PV (HPV).

Declaration of conflicting interests

The author(s) declared no potential conflicts of interests with respect to the research, authorship, and/or publication of this article.

Funding

The author(s) disclosed receipt of the following financial support for the research, authorship, and/or publication of this article: This research was partially supported by Regione Campania and Regione Basilicata. The funders of the work did not influence study design, data collection and analysis, decision to publish, or preparation of the manuscript.

Acknowledgements

We would like to thank prof. D. DiMaio, Yale University, New Haven, for kindly providing us an anti-E5 rabbit polyclonal antiserum; Dr. L. Nasir, Glasgow University, Glasgow, for kindly providing us a polyclonal sheep anti-E5 antibody; Dr. P. Sarnelli, Regione Campania, Dr G. Salvatore, Regione Basilicata and Dr S. Morace, Catanzaro University “Magna Graecia” for their technical help.

Appendix A. Supplementary data

Supplementary material related to this article can be found, in the online version, at doi:https://doi.org/10.1016/j.vetmic.2019.04.021.

References

Behl, C., 2011. Bag3 and friends. Co-chaperones in selective autophagy during aging and disease. Autophagy 7, 795–798.
Behl, C., 2016. Breaking BAG: the co-chaperone BAG3 in health and disease. Trends Pharmacol. Sci. 37, 672–688.
Campo, M.S., 2003. Papillomavirus and disease in humans and animals. Vet. Comp. Oncol. 1, 3–14.
Campo, M.S., Jarrett, W.F.H., Barron, R.J., O'Neilm, B.W., Smith, K.T., 1992. Association of bovine papillomavirus type 2 and bracken fern with bladder cancer in cattle. Cancer Res. 52, 6898–6904.
Carchman, E.H., Matkowskyj, K.A., Meske, L., Lambert, P.F., 2016. Dysregulation of autophagy contributes to anal carcinogenesis. PLoS One 11 (10), e0164273.
Carra, S., 2009. The stress-inducible HspB8-Bag3 complex induces the eIF2α kinase

pathway. Autophagy 5, 428–429.
Carra, S., Seguin, S.M., Landry, J., 2008. HspB8 and Bag3. Autophagy 4, 237–239.
Carra, S., Brunsting, J.F., Lambert, H., Landry, J., Kampinga, H.H., 2009. HspB8 participates in protein quality control by a non-chaperone-like mechanism that requires eIF2α phosphorylation. J. Biol. Chem. 284, 5523–5532.
Choi, Y., Bowman, J.W., Jung, J.U., 2018. Autophagy during viral infection – a double-edged sword. Nat. Rev. Microbiol. 16, 341–354.
Daudt, C., Da Silva, F.R.C., Lunardi, M., Alves, C.B.D.T., Weber, M.N., Cibulski, S.P., Alfieri, A.F., Alfieri, A.A., Canal, C.W., 2018. Papillomavirus in ruminants: an update. Transbound. Emerg. Dis. 65, 1381–1395.
DeMasi, J., Chao, M.C., Kumar, A.S., Howley, P.M., 2007. Bovine papillomavirus E7 oncoprotein inhibits anoikis. J. Virol. 81, 9419–9425.
Deretic, V., Saitoh, T., Akira, S., 2013. Autophagy in infection, inflammation, and immunity. Nat. Rev. Immunol. 13, 722–737.
Dice, J.F., 2007. Chaperone-mediated autophagy. Autophagy 3, 295–299.
DiMaio, D., Petti, L., 2013. The E5 proteins. Virology 445, 99–114.
Donnelly, N., Gorman, A.M., Gupta, S., Samali, A., 2013. The eIF2α kinases: their structures and functions. Cell. Mol. Life Sci. 70, 3493–3511.
Gamerdinger, M., Carra, S., Behl, C., 2011a. Emerging role of molecular chaperones and co-chaperones in selective autophagy: focus on BAG proteins. J. Mol. Med. 89, 1175–1182.
Gamerdinger, M., Kaya, A.M., Wolfrum, U., Clement, A.M., Behl, C., 2011b. BAG3 mediates chaperone-based aggresome-targeting and selective autophagy of misfolded proteins. EMBO Rep. 12, 149–156.
Griffin, L.M., Cicchini, L., Pyeon, D., 2013. Human papillomavirus infection is inhibited by host autophagy in primary human keratinocytes. Virology 437, 12–19.
Guilbert, S.M., Lambert, H., Rodrigue, M.A., Fuchs, M., Landry, J., Lavoie, J.N., 2018. HSPB8 and BAG3 cooperate to promote spatial sequestration of ubiquitinated proteins and coordinate the cellular adaptive response to proteasome insufficiency. FASEB J. 32, 3518–3535.
Ichimura, Y., Komatsu, K., 2010. Selective degradation of p62 by autophagy. Semin. Immunopathol. 32, 431–436.
Jaakkola, P.M., Pursiheimo, J.P., 2009. P62 degradation by autophagy. Autophagy 5, 410–412.
Jia, B., Wu, Y., Zhou, Y., 2014. 14-3-3 and aggresome formation: implications in neurodegenerative diseases. Prion 28123 Epub 2014 Feb 18.
Katsuragi, Y., Ichimura, Y., Komatsu, M., 2015. P62/SQSTM1 functions as a signaling hub and an autophagy adaptor. FEBS J. 282, 4672–4678.
Kazemi, S., Papadopoulou, S., Li, S., Su, O., Wang, S., Yoshimura, A., Matlashewski, G., Dever, T.E., Koromilas, A.E., 2004. Control of α subunit of eukaryotic translation initiation factor 2 (eIF2α) phosphorylation by the human papillomavirus type 18 E6 oncoprotein: implications for eIF2α-dependent gene expression and cell death. Mol. Cell. Biol. 24, 3415–3429.
Kettern, N., Rogon, C., Limmer, A., Schild, H., Höhfeld, J., 2011. The Hsc/Hsp70 co-chaperone network controls antigen aggregation and presentation during maturation of professional antigen presenting cells. PLoS One 6 (1), e16398.
Klimek, C., Kathage, B., Wörderhoff, J., Höhfeld, J., 2017. BAG3-mediated proteostasis at a glance. J. Cell. Sci. 130, 2781–2788.
Lee, Y.R., Kuo, S.H., Lin, C.Y., Fu, P.J., Yeh, T.M., Liu, H.S., 2018. Dengue virus-induced ER stress is required for autophagy activation, viral replication, and pathogenesis both *in vitro* and in vivo. Sci. Rep. 8, 489. https://doi.org/10.1038/s41598-017-18909-3.
Li, X., Gong, Z., Zhang, L., Zhao, C., Zhao, X., Gu, X., Chen, H., 2015. Autophagy knocked down by high-risk HPV infection and uterine cervical carcinogenesis. Int. J. Clin. Exp. Med. 8, 10304–10314.
Li, X.C., Hu, Q.K., Chen, L., Liu, S.Y., Su, S., Tao, H., Zhang, L.N., Sun, T., He, L.J., 2017. HSPB8 promotes the fusion of autophagosome and lysosome during autophagy in diabetic neurons. Int. J. Med. Sci. 14, 1335–1341.
Ling, Y., Zhang, X., Qi, G., Yang, S., Jingjiao, L., Shen, Q., Wang, X., Cui, L., Hua, X., Deng, X., Delwart, E., Zhang, W., 2019. Viral metagenomics reveals significant viruses in the genital tract of apparently healthy dairy cows. Arch. Virol. 164, 1059–1167.
Maiolino, P., Ozkul, A., Sepici-Dincel, A., Roperto, F., Yücel, G., Russo, V., Urraro, C., Lucà, R., Riccardi, M.C., Martano, M., Borzacchiello, G., Esposito, I., Roperto, S., 2013. Bovine papillomavirus type 2 infection and microscopic patterns of urothelial tumors of the urinary bladder in water buffaloes. Biomed Res. Int. 937918. https://doi.org/10.1155/2013/937918.
Mattoscio, D., Medda, A., Chiocca, S., 2018. Human papilloma virus and autophagy. Int. J. Mol. Sci. 19, 1775. https://doi.org/10.3390/ijms19061775.
McKenney, R.J., Huynh, W., Tanenbaum, M.E., Bhabha, G., Vale, R.D., 2014. Activation of cytoplasmic dynein motility by dynactin-cargo adapter complexes. Science 6194, 337–341. https://doi.org/10.1126/science. 1254198, Epub 2014 Jun 19.
Mizushima, N., Levine, B., 2010. Autophagy in mammalian development and differentiation. Nat. Cell Biol. 12, 823–830.
Park, J., Park, Y., Ryu, I., Choi, M.H., Lee, H.J., Oh, N., Kim, K., Kim, K.M., Choe, J., Lee, C., Baik, J.H., Kim, Y.K., 2017. Misfolded polypeptides are selectively recognized and transported toward aggresomes by a CED complex. Nat Commun Jun 7 (8), 15730. https://doi.org/10.1038/ncomms1573.
Park, Y., Park, J., YK, 2018. Kim. Crosstalk between translation and the aggresome–autophagy pathway. Autophagy 14 (6), 1079–1081. https://doi.org/10.1080/15548627.2017. 1358849, Epub 2017 Nov 23.
Pamukcu, A.M., 1974. Tumours of the urinary bladder. Bull. Wld. Health Org. 50, 43–52.
Pankiv, S., Clausen, T.H., Lamark, T., Brech, A., Bruun, J.A., Outzen, H., Øvervatn, A., Bjørkøy, G., Johansen, T., 2007. p62/SQSTM1 binds directly to Atg8/LC3 to facilitate degradation of ubiquitinated protein aggregates by autophagy. J. Biol. Chem. 287, 24131–24145.
Rapino, F., Jung, M., Fulda, S., 2014. BAG3 induction is required to mitigate proteotoxicity via selective autophagy following inhibition of constitutive protein degradation pathways. Oncogene 33, 1723–1724.
Ron, D., Harding, H.P., 2012. Protein-folding homeostasis in the endoplasmic reticulum and nutritional regulation. Cold Spring Harb. Perspect. Biol. 4, a013177.
Roperto, S., Borzacchiello, G., Brun, R., Leonardi, L., Maiolino, P., Martano, M., Paciello, O., Papparella, S., Restucci, B., Russo, V., Salvatore, G., Urraro, C., Roperto, F., 2010a. A review of bovine urothelial tumours and tumour-like lesions of the urinary bladder. J. Comp. Pathol. 142, 95–108.
Roperto, S., De Tullio, R., Raso, C., Stifanese, R., Russo, V., Gaspari, M., Borzacchiello, G., Averna, M., Paciello, O., Cuda, G., Roperto, F., 2010b. Calpain3 is expressed in a proteolytically active form in papillomavirus-associated urothelial tumors of the urinary bladder in cattle. PLoS One 5 (4), e10299.
Roperto, S., Russo, V., Ozkul, A., Corteggio, A., Sepici-Dincel, A., Catoi, C., Esposito, I., Ricciardi, M.G., Urraro, C., Lucà, R., Ceccarelli, D.M., Longo, M., Roperto, F., 2013. Productive infection of bovine papillomavirus type 2 in the urothelial cells of naturally occurring urinary bladder tumors in cattle and water buffaloes. PLoS One 8 (5), e62227.
Roperto, S., Russo, V., Leonardi, L., Martano, M., Corrado, F., Riccardi, M.G., Roperto, F., 2016. Bovine papillomavirus type 13 expression in the urothelial bladder tumours of cattle. Transbound. Emerg. Dis. 63, 628–634.
Roperto, S., Russo, V., Corrado, F., De Falco, F., Munday, J.S., Roperto, F., 2018a. Oral fibropapillomatosis and epidermal hyperplasia of the lip in newborn lambs associated with bovine Deltapapillomavirus. Sci. Rep. 8, 13310. https://doi.org/10.1038/s41598-018-31529-9.
Roperto, S., Russo, V., Rosati, A., Ceccarelli, D.M., Munday, J.S., Turco, M.C., Roperto, F., 2018b. Chaperone-assisted selective autophagy in healthy and papillomavirus-associated neoplastic urothelium of cattle. Vet. Microbiol. 221, 134–142.
Sannigrahi, M.K., Singh, V., Sharma, R., Panda, N.K., Khullar, M., 2015. Role of autophagy in head and neck cancer and therapeutic resistance. Oral Dis. 21, 283–291.
Schlegel, R., Wade-Glass, M., Rabson, M.S., Yang, Y.C., 1986. The E5 transforming gene of bovine papillomavirus encodes a small hydrophobic protein. Science 233, 464–467.
Shen, S., Niso-Santano, M., Adjemian, S., Takehara, T., Malik, S.A., Minoux, H., Souquere, S., Mariño, G., Lachkar, S., Senovilla, L., Galluzzi, L., Keep, O., Pierron, G., Maiuri, M.C., Hikita, H., Kroemer, R., 2012. Cytoplasmic STAT3 represses autophagy by inhibiting PKR activity. Mol. Cell 48, 667–680.
Sturnër, E., Behl, C., 2017. The role of the multifunctional BAG3 protein in cellular protein quality control and in disease. Front. Mol. Neurosci. 10https://doi.org/10.3389/fnmol.2017.00177. art 177.
Surviladze, Z., Sterk, R.T., DeHaro, S.A., Ozbun, M.A., 2013. Cellular entry of human papillomavirus type 16 involves activation of the phosphatidylinositol 3-kinase/Akt/mTOR pathway and inhibition of autophagy. J. Virol. 87, 2508–2517.
Tallóczy, Z., Jiang, W., Virgin IV, H.W., Leib, D.A., Scheuner, D., Kaufman, R.J., Eskelinen, E.L., Levine, B., 2002. Regulation of starvation- and virus-induced autophagy by the eIF2α kinase signalling pathway. Proc. Natl. Acad. Sci. U. S. A. 99, 190–195.
Ulbricht, A., Eppler, F.J., Tapia, V.E., van der Ven, P.F., Hampe, N., Hersch, N., Vakeel, P., Stadel, D., Haas, A., Saftig, P., Behrends, C., Fürst, D.O., Wolkmer, R., Hoffmann, B., Kolanus, W., Höhfeld, J., 2013. Cellular mechanotransduction relies on tension-induced and chaperone-assisted autophagy. Curr. Biol. 23, 430–435.
Venuti, A., Paolini, F., Nasir, L., Corteggio, A., Roperto, S., Campo, M.S., Borzacchiello, G., 2011. Papillomavirus E5: the smallest oncoprotein with many functions. Mol. Cancer 10, 140. https://doi.org/10.1186/1476-4598-10-140.
Wang, H.I., Yang, G.F., Huang, Y.H., Huang, Q.W., Gao, J., Zhao, X.D., Huang, L.M., Chen, H.L., 2014. Reduced expression of autophagy markers correlates with high-risk human papillomavirus infection in human cervical squamous cell carcinoma. Oncol. Lett. 8, 1492–1498.